Biochemical and Biophysical Research Communications 463 (2015) 551–556

Contents lists available at ScienceDirect

Biochemical and Biophysical Research Communications

journal homepage: www.elsevier.com/locate/ybbrc

The PARP1 inhibitor BMN 673 exhibits immunoregulatory effects in a *Brca1*$^{-/-}$ murine model of ovarian cancer

Jing Huang [a, b, 1], Lei Wang [a, 1], Zhongyi Cong [a, c], Zohreh Amoozgar [a, d], Evgeny Kiner [a], Deyin Xing [e], Sandra Orsulic [f], Ursula Matulonis [g], Michael S. Goldberg [a, *]

[a] Department of Cancer Immunology and AIDS, Dana-Farber Cancer Institute, Boston, MA, USA
[b] Department of Immunology, School of Basic Medical Sciences, Peking University, Beijing, China
[c] Department of Regenerative Medicine, School of Pharmaceutical Sciences, Jilin University, Changchun, China
[d] Department of Radiation Oncology, Massachusetts General Hospital, Boston, MA, USA
[e] Department of Pathology, Johns Hopkins University, Baltimore, MD, USA
[f] Women's Cancer Program, Samuel Oschin Comprehensive Cancer Institute, Cedars-Sinai Medical Center, Los Angeles, CA, USA
[g] Gynecologic Oncology Program, Dana-Farber Cancer Institute, Boston, MA, USA

ARTICLE INFO

Article history:
Received 13 May 2015
Accepted 17 May 2015
Available online 3 June 2015

Keywords:
BMN 673
PARP1
Ovarian cancer
Immune microenvironment

ABSTRACT

Familial breast and ovarian cancer are often caused by inherited mutations of *BRCA1*. While current prognoses for such patients are rather poor, inhibition of poly-ADP ribose polymerase 1 (PARP1) induces synthetic lethality in cells that are defective in homologous recombination. BMN 673 is a potent PARP1 inhibitor that is being clinically evaluated for treatment of *BRCA*-mutant cancers. Using the *Brca1*-deficient murine epithelial ovarian cancer cell line BR5FVB1-Akt, we investigated whether the antitumor effects of BMN 673 extend beyond its known pro-apoptotic function. Administration of modest amounts of BMN 673 greatly improved the survival of mice bearing subcutaneous or intraperitoneal tumors. We thus hypothesized that BMN 673 may influence the composition and function of immune cells in the tumor microenvironment. Indeed, BMN 673 significantly increases the number of peritoneal $CD8^+$ T cells and NK cells as well as their production of IFN-γ and TNF-α. These data suggest that the cell stress caused by BMN 673 induces not only cancer cell-intrinsic apoptosis but also cancer cell-extrinsic antitumor immune effects in a syngeneic murine model of ovarian cancer. BMN 673 may therefore serve as a promising adjuvant therapy to immunotherapy to achieve durable responses among patients whose tumors harbor defects in homologous recombination.

1. Introduction

Ovarian cancer is the leading cause of death from gynaecological malignancies, with an overall mortality of 60% [1]. Treatment of epithelial ovarian cancer is based on the combination of cytoreductive surgery and platinum/taxane-based chemotherapy [2], which are invasive and toxic, respectively. Molecular targeted agents, such as Poly (ADP-ribose) polymerase (PARP) inhibitors, represent an exciting new avenue of clinical investigation [3,4]. Inhibition of PARP1, which is involved in DNA base excision repair selectively kills cancer cells harboring dysfunctional homologous recombination, which is a hallmark of BRCA1/2-deficient tumors [5,6].

BMN 673, (8S,9R)-5-fluoro-8-(4-fluorophenyl)-9-(1-methyl-1H-1,2,4-triazol-5- yl)-8,9-dihydro-2H-pyrido[4,3,2-de]-phthalazin-3(7H)-one, is a highly potent PARP1 inhibitor, with a reported IC50 of 0.57 nM [7]. While other PARP inhibitors – such as rucaparib, veliparib and olaparib – similarly inhibit PARP catalytic activity at nanomolar concentrations, BMN 673 confers a cytotoxic potency that exceeds those of other PARP inhibitors by a factor of 10-fold or greater [8]. BMN 673 is thus the most potent PARP inhibitor in clinical development, and its enhanced efficacy may be attributable to its capacity to trap PARP-DNA complexes [7,8]. Its impressive antitumor activity is associated with limited toxicity in BRCA-deficient breast and ovarian cancer patients [9] as well as a subset of lung cancer patients [10].

* Corresponding author.
E-mail address: michael_goldberg1@dfci.harvard.edu (M.S. Goldberg).
[1] These authors contributed equally to this work.

http://dx.doi.org/10.1016/j.bbrc.2015.05.083
0006-291X/

Ovarian cancer is characterized by a progressive peritoneal ascites and a highly immunosuppressive tumor microenvironment. Despite modest improvements in progression-free and median survival using combination chemotherapy, overall survival rates for patients with advanced epithelial ovarian cancer remain disappointingly low. Preclinical and clinical studies suggest that the ovarian tumor microenvironment contributes to tumor progression, metastasis, and chemotherapy resistance [11,12]. Therefore, therapies that not only kill cancer cells but also modify the local microenvironment are worthy of investigation. Specifically, the ability to recruit and activate cytotoxic lymphocytes can lead to antitumor immunity.

In this study, we use the *Brca1*$^{-/-}$ murine ovarian cancer cell line BR5FVB1-Akt, which has been shown to recapitulate critical characteristics of human epithelial ovarian cancer. With this model, we provide the first *in vitro* and *in vivo* analysis of BMN 673 function in a murine ovarian cancer model and confirm its ability to induce apoptosis specifically in the context of *Brca1* deficiency. We inspect its impact on the immune microenvironment, and our data suggest that BMN 673 may thereby promote the development of antitumor immunity.

2. Materials and methods

2.1. Drugs and tumor cell lines

BMN 673 was obtained from Selleckchem (Houston, TX). BR5FVB1-Akt (*Brca*$^{-/-}$ murine ovarian carcinoma) cells were generated as described previously [13]. ID8- Vegf (*Brca*$^{+/+}$ murine ovarian carcinoma) cells were provided by Dr. Jose Conejo-Garcia (The Wistar Institute, Philadelphia, PA) and have been described previously [14]. BR5FVB1-Akt and ID8-Vegf cells were maintained in DMEM and RPMI-1640 media (Invitrogen, Carlsbad, CA), respectively, supplemented with 10% fetal bovine serum (FBS), 2 mM L-glutamine, and 100 U/ml penicillin/streptomycin (Roche, Indianapolis, IN) in a 5% CO_2 atmosphere at 37 °C. 0.5 mM sodium pyruvate and 3.4 μl/L of β-mercaptoethanol were also added to the ID8-Vegf media.

2.2. Flow cytometry analysis of cell apoptosis

BR5FVB1-Akt and ID8-Vegf cells were seeded into 12-well plates at a density of 40,000 cells per well and incubated overnight in 1 ml of complete media. The media was replaced with 1 ml of fresh media and supplemented with BMN 673 to concentrations of 0.1, 1, 10, and 100 nM for either 48 or 72 h. Cells were collected and washed once with ice-cold phosphate-buffered saline (PBS). Cell pellets were stained with APC-conjugated Annexin V and propidium iodide according to the manufacturer's protocol (eBioscience, San Diego, CA). Analyses were performed on a FACS-Caliber (BD Biosciences) with CELLQuest software.

2.3. Cell viability assay

BR5FVB1-Akt and ID8-Vegf cells were plated at a density of 10,000 cells per well in 96-well plates in 100 μl complete media. The cells were treated with BMN 673 at increasing concentrations (0, 0.1, 1, 10, and 100 nM) for 0, 24, 48 and 72 h. After the appropriate incubation time, cell viability was evaluated using the CCK8 assay kit (Dojindo Laboratories, Tokyo, Japan) according to the manufacturer's instructions, and absorbance was read at 450 nm using a PerkinElmer 1420 VICTOR 3V multilabel counter (PerkinElmer, Waltham, MA, USA).

2.4. Animal model and drug treatment

All animal procedures were performed in compliance with protocols approved by the Institutional Animal Care and Use Committee of Dana-Farber Cancer Institute. Six-week-old female FVB mice were obtained from Charles River Laboratory (Boston, MA, USA) and kept in a dedicated animal facility with five mice per cage.

For *in vivo* experiments, intraperitoneal (i.p.) and subcutaneous (s.c.) murine tumors were established. To generate i.p. tumors, six-week-old female FVB mice were injected i.p. with a total volume of 400 μl opti-MEM containing 4×10^6 BR5FVB1-Akt cells. Beginning four days after i.p. inoculation of cancer cells, the mice ($n = 5$) were administered BMN 673 (20 mM DMSO stock solution diluted in PBS for a total volume of 100 μl per mice) or solvent control (DMSO/PBS mix) via i.p. injection every other day for a total of five doses. The mice were subsequently monitored for health deterioration and sacrificed upon ascites development.

To generate murine s.c. tumors, 6×10^6 BR5FVB1-Akt cells in 500 μl opti-MEM media were injected s.c. into the back flank of six-week-old female FVB mice. Beginning four days after s.c. inoculation of cancer cells, the mice ($n = 5$) were administered BMN 673 (1 mg/kg) or solvent control (DMSO/PBS mix) via i.p. injection every other day for a total of five doses. Established tumors were apparent by day 22. Briefly, tumor volumes were determined by measuring the major (L) and minor (W) diameters with an electronic caliper. The tumor volume was calculated according to the following formula: tumor volume $= 2/L \times W^2$. *$p < 0.05$, versus DMSO control.

2.5. Flow cytometric analysis of tumor-associated leukocytes

BR5FVB1-Akt cells (4×10^6) were injected i.p. into mice ($n = 7$), and the animals were sacrificed on day 24 post-injection. Five ml of PBS were injected into the peritoneal cavity, and the i.p. fluid was collected. The cells in the i.p. fluid are defined as tumor-associated leukocytes (TALs). For surface marker staining, the TALs were stained with PE/Cy7-conjugated anti-mouse CD3, phycoerythrin (PE)-conjugated anti-mouse CD4, Percp-Cy5.5-conjugated anti-mouse CD8, APC-conjugated anti-mouse Nkp46, eFluor 450-conjugated anti-mouse CD19, fluorescein isothiocyanate (FITC)-conjugated anti-mouse Gr1, PE-conjugated anti-mouse Ly6G, APC-conjugated anti-mouse F4/80, Percp-Cy5.5-conjugated anti-mouse CD11c, or APC/Cy7-conjugated anti-mouse CD11b (Biolegend, San Diego, CA).

For intracellular cytokine staining, the TALs were stimulated with 20 ng/ml phorbol 12-myristate 13-acetate (PMA) and 1 μg/ml ionomycin for 6 h, followed by addition of Brefeldin-A (eBioscience, San Diego, CA) into the media for 2 h. Cells were scraped and washed in FACS buffer (PBS supplemented with 2% FBS). Cells were first stained with surface markers, fixed, and then permeabilized with Cytofix/Cytoperm buffer. Next, a single-cell suspension was passed through a 70 μm mesh to remove possible cellular aggregates. Intracellular staining was performed using FITC-conjugated anti-mouse Foxp3, FITC-conjugated anti-mouse IFN-γ, and PE-conjugated anti-mouse TNF-α (Biolegend, San Diego, CA).

A total of 50,000 events were recorded per sample with CELLQuest software on a BD FACSAria. Data were analyzed using FlowJo software.

2.6. Quantitative real-time PCR analysis

qPCR was used to examine the impact of BMN 673 treatment on the expression of immunoregulatory genes known to be important in ovarian cancer. BR5FVB1-Akt cells were treated with BMN 673 or DMSO for 72 h. Relative gene expression was measured using the

Ambion® Cells-to-CT™ Kit 1-Step Power SYBR® Green Kit (Life Technologies, Carlsbad, CA) on an Applied Biosystems 7500 real-time PCR system. qPCR assays were performed in technical triplicate with biological duplicate.

2.7. Statistical analysis

Statistical analysis was performed with GraphPad Prism 5 (La Jolla, CA, USA). Statistical significance among groups was determined by a Student t test and one-way ANOVA. Survival groups were compared using a Mantel–Cox test. Samples were considered to be significantly different if $p < 0.05$.

3. Results

3.1. BMN 673 is cytotoxic to $Brca^{-/-}$ but not $Brca^{+/+}$ ovarian cancer cells

Consistent with the proposed mechanism of synthetic lethality, we found that BMN 673 inhibited the proliferation of $Brca1^{-/-}$ BR5FVB1-Akt cells in a dose-dependent manner but had no effect on $Brca^{+/+}$ ID8-Vegf cells (Fig. 1A). We showed that the growth defect was attributable to induction of apoptosis, as evidenced by flow cytometric analysis. After 72 h of treatment with BMN 673 (0.1, 1, 10, or 100 nM), the percentage of apoptotic cells increased 5–20% over DMSO control in BR5FVB1-Akt cells, but no obvious changes were observed in ID8-Vegf cells treated with BMN 673 (Fig. 1B,C).

We confirmed that the effects of BMN 673 results extend to human ovarian cancer cells, observing similar anti-proliferative and pro-apoptotic effects in *BRCA1*-promoter hypermethylated OVCAR8 cells but not in *BRCA1*-wild type SKOV3 cells (Supplemental Fig. 1). We then compared the efficacy of BMN 673 with that of olaparib, a PARP inhibitor that has previously been characterized in preclinical models of ovarian cancer [15], and determined that BMN 673 inhibits cell proliferation to a greater extent than olaparib (Supplemental Fig. 2), suggesting greater *in vitro* potency.

3.2. BMN 673 potently inhibits tumorigenicity

The therapeutic potential of BMN 673 was subsequently examined *in vivo*, using subcutaneous and orthotopic syngeneic tumor models. First, BR5FVB1-Akt cells were inoculated subcutaneously into FVB mice, and BMN 673 was administered at a dose of 1.0 mg/kg via intraperitoneal (i.p.) injection on days 4, 6, 8, 10, and

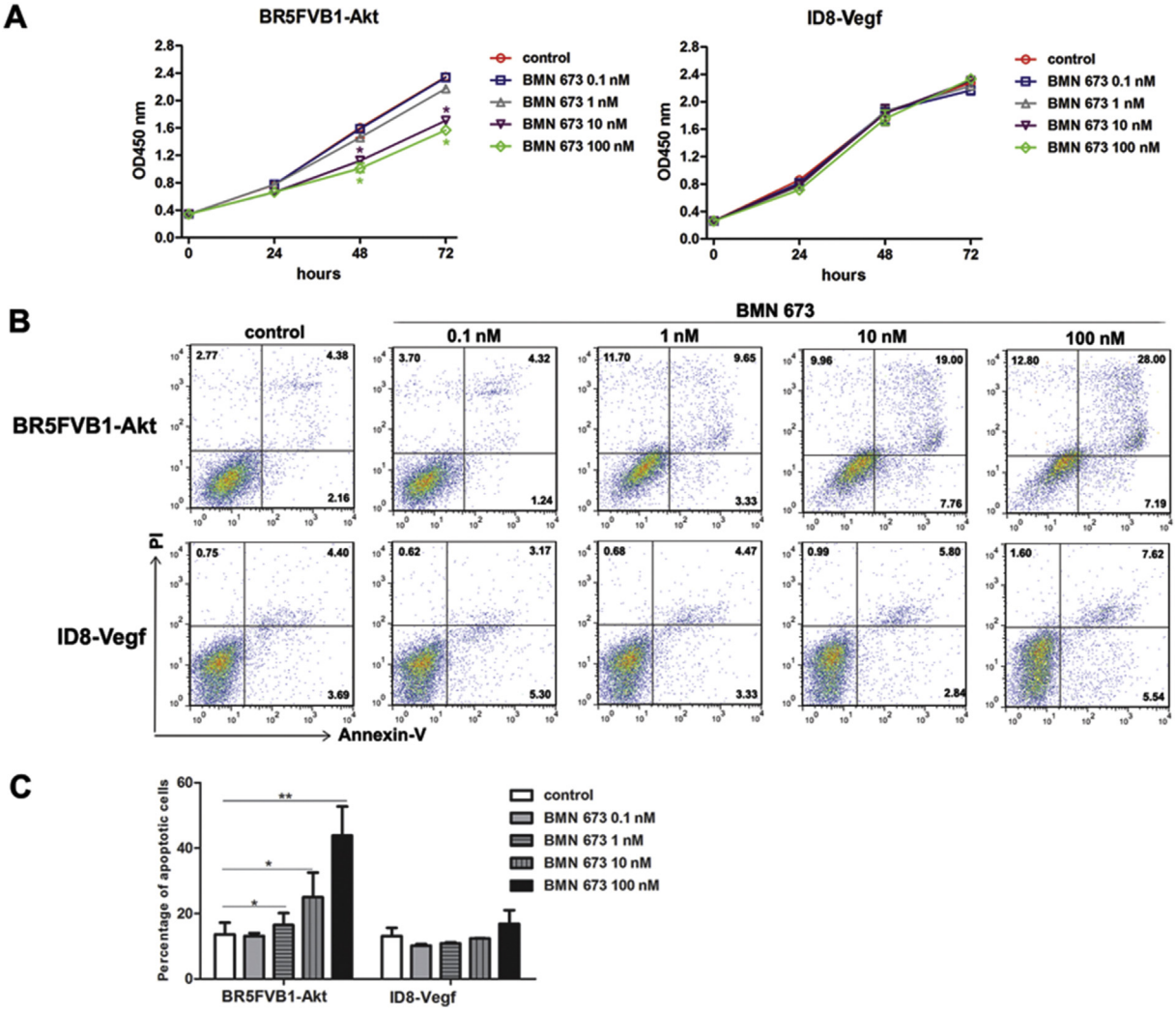

Fig. 1. BMN 673 inhibits cell proliferation and induces apoptosis specifically in the context of *Brca1* deficiency. BR5FVB1-Akt and ID8-Vegf cells were treated with BMN 673 at designated concentrations and **(A)** cell proliferation and **(B)** cell apoptosis were analyzed. **(C)** The precentage of apoptotic cells are shown for DMSO control- and BMN 673-treated cells. Data are means ± SD of triplicate independent treatment for each time point. $^{*}p < 0.05$, $^{**}p < 0.01$ versus DMSO control (t-test).

12 post tumor inoculation. Tumors in mice receiving BMN 673 exhibited a significant reduction in growth relative to control mice, with 80% of mice achieving a complete response, as evidenced by a lack of palpable tumor (Fig. 2A). Next, BR5FVB1-Akt cells were inoculated i.p. into FVB mice, and BMN 673 was administered i.p. at a dose of 0.1, 0.25, 0.5, 1.0 or 2.5 mg/kg on days 4, 6, 8, 10, and 12 post tumor inoculation. BMN 673 significantly improved mouse survival relative to DMSO control, even at very low doses. A dose of 1.0 mg/kg was curative to all mice and was well tolerated, as evidenced by a lack of weight loss (Fig. 2B). In both settings, only five doses were administered on alternating days, which is considerably less than the twice daily oral gavage for 28 consecutive days previously reported in an immunodeficient model [7]. We thus sought to determine whether the observed efficacy may have been mediated in part by immune stimulation.

3.3. BMN 673 treatment alters the composition of tumor-associated leukocytes

We were thus interested to assess whether BMN 673 treatment yields immunomodulatory effects *in vivo*. Orthotopic tumors were generated, and tumor-bearing mice were treated with DMSO control or BMN 673 as above. On day 24 post-inoculation, peritoneal fluid was collected and TALs were analyzed. Representative figures of flow cytometric analysis of $CD4^+$T cells, $CD8^+$ T cells, B cells, NK cells, $CD4^+$ regulatory T cells (Tregs), tumor-associated macrophages (TAMs) and myeloid-derived suppressor cells (MDSCs) are shown in Fig. 3A. The percentages of $CD8^+$ cytotoxic T lymphocytes (BMN 673 23.37% vs. control 13.36%, $p = 0.017$), B cells (BMN 673 77% vs. control 64.4%, $p = 0.004$), and NK cells (BMN 673 1.824% vs. control 0.671%, $p = 0.0002$) significantly increased in BMN 673 treated-mice compared to those in control mice.

Recently, it has been shown that high expression of the lymphocyte-recruiting chemokines CCL2 and CCL5 is associated with the presence of TILs in ovarian cancer [16]. For this reason, we hypothesized that BMN 673 may induce the expression of these chemokines. Quantitative real-time PCR data confirm that this drug upregulates these immunomodulatory genes in a dose-dependent manner (Supplemental Fig. 3), providing insight into the mechanism of lymphocyte homing following BMN 673 treatment.

Whereas the percentage of antitumor immune cells increased, the percentage of immunosuppressive cells differed between the lymphocyte and myeloid populations. The percentage of Tregs was increased (BMN 673 5.096% vs. control 3.056%, $p = 0.0199$), while the percentage of MDSCs was decreased (BMN 673 0.1773% vs. control 0.8611%, $p = 0.0169$) in BMN 673-treated mice relative to control mice (Fig. 3B). The percentages of macrophages and $CD4^+$ T helper cells did not differ significantly, nor did the, $CD8^+$/Treg ratio.

3.4. BMN 673 treatment enhances the function of tumor-associated leukocytes

To elucidate the functional capacity of effector leukocytes in the tumor environment, we evaluated the expression levels of IFN-γ and TNF-α among $CD8^+$ cytotoxic T lymphocytes, NK cells, and macrophages recovered from control- or BMN 673- treated mice. Representative figures of flow cytometric analysis of these immune effector molecules are shown in Fig. 4A. The expression of both IFN-γ and TNF-α was significantly upregulated in both lymphocyte populations after BMN 673 treatment, though no obvious changes were observed in macrophages (Fig. 4B). These data suggest that BMN 673 treatment not only recruits antitumor immune cells but also promotes their antitumor function in the tumor microenvironment.

4. Discussion

In the study reported herein, we tested the antitumor activity of the novel PARP inhibitor BMN 673 in ovarian cancer cell lines and animal models. Our data indicate that BMN 673 has antiproliferative and pro-apoptotic effects on a *Brca1*-deficient murine ovarian cancer cell line. ID8-Vegf cells, which are *Brca1* wild

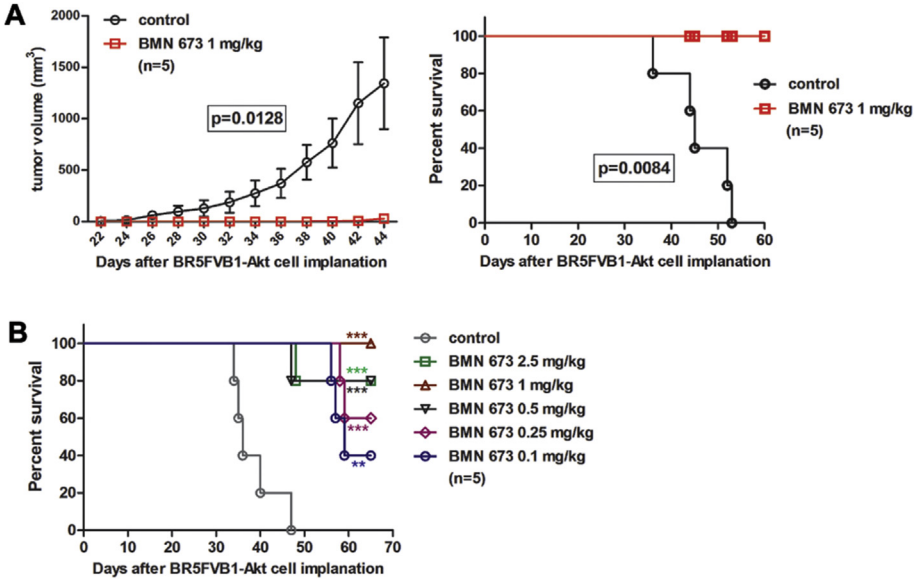

Fig. 2. BMN 673 inhibits tumor growth and extends survival among FVB mice bearing syngeneic BR5FVB1-Akt ovarian tumors. (A) *In vivo* subcutaneous anti-tumor assay. 6×10^6 BR5FVB1-Akt cells were subcutaneously injected into mice ($n = 5$ per group), which were injected i.p. with 1 mg/kg BMN 673 on days 4, 6, 8, 10, and 12. Tumor volumes were measured at the indicated time points (left). Mouse survival was monitored over time and analyzed using the Log-rank test (right). **(B)** *In vivo* orthotopic anti-tumor assay. Kaplan–Meier survival curve of mice ($n = 5$ per group) following i.p. inoculation of 4×10^6 BR5FVB1-Akt cells and subsequent i.p. injection of BMN 673 (0.1, 0.25, 0.5, 1, or 2.5 mg/kg) on days 4, 6, 8, 10, and 12. Survival was monitored over time and analyzed using the Log-rank test; $^{**}p < 0.01$, $^{***}p < 0.001$, versus DMSO control. The experiment was halted on day 66, which represnts a doubling of the median survival for DMSO control-treated mice.

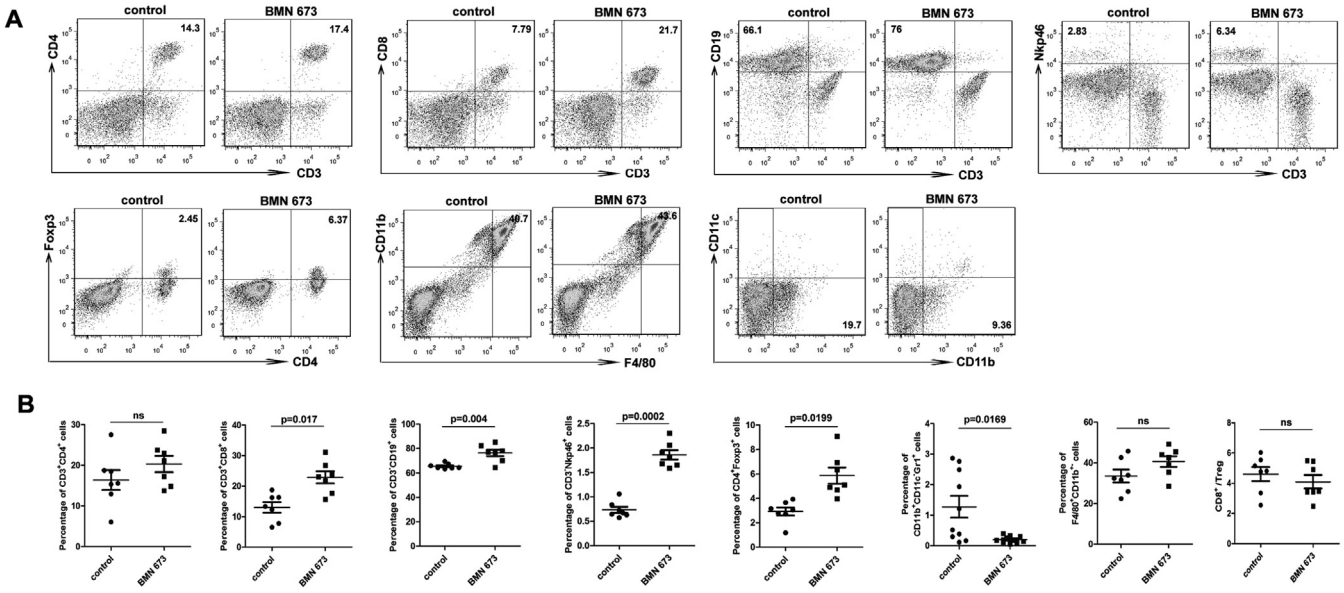

Fig. 3. BMN 673 treatment alters the balance of immune cells in the peritoneal ascites of tumor-bearing mice. FVB mice were inoculated i.p. with 4×10^6 BR5FVB1-Akt cells and then treated i.p. with PBS or 1 mg/kg BMN 673 on days 4, 6, 8, 10, and 12. On day 24 post tumor inoculation, a peritoneal wash was performed, and single-cell suspensions were analyzed by flow cytometry. **(A)** Representative figures of flow cytometric analyses of TALs from DMSO control- and BMN 673-treated mice. **(B)** Quantitation of results from A with statistical results. ns: not significant.

type, are unaffected by BMN 673 treatment, confirming that the drug is an on-target PARP1 inhibitor. The synthetic lethal phenotype can be observed in any cell that exhibits defective homologous recombination, whether it is caused by germline or somatic *BRCA1* or *BRCA2* mutations, *BRCA1* promoter methylation, or other genetic and epigenetic abnormalities of genes involved in homologous recombination [17]. We confirmed that BMN 673 is at least 10-fold more potent than olaparib in BR5FVB1-Akt cells. While these findings were consistent with previous studies, the effects of BMN 673 had not yet been reported in an immunocompetent cancer model.

Our data demonstrate that BMN 673 confers significant therapeutic efficacy in immunocompetent ovarian tumor-bearing mice. We observed that BMN 673 influences the composition and function of tumor-associated leukocytes in the periotneal cavity. The percentages of cytotoxic $CD8^+$ T cells, B cells, and NK cells were increased, while the percentage of immunosuppressive MDSCs decreased. Many studies have shown that MDSCs promote tumor progression via multiple suppressive mechanisms [18]. In contrast, the presence of cytotoxic immune cells, such as cytotoxic $CD8^+$ T cells and NK cells, within the tumor microenvironment is associated with a good prognosis in ovarian cancer [19,20]. Moreover,

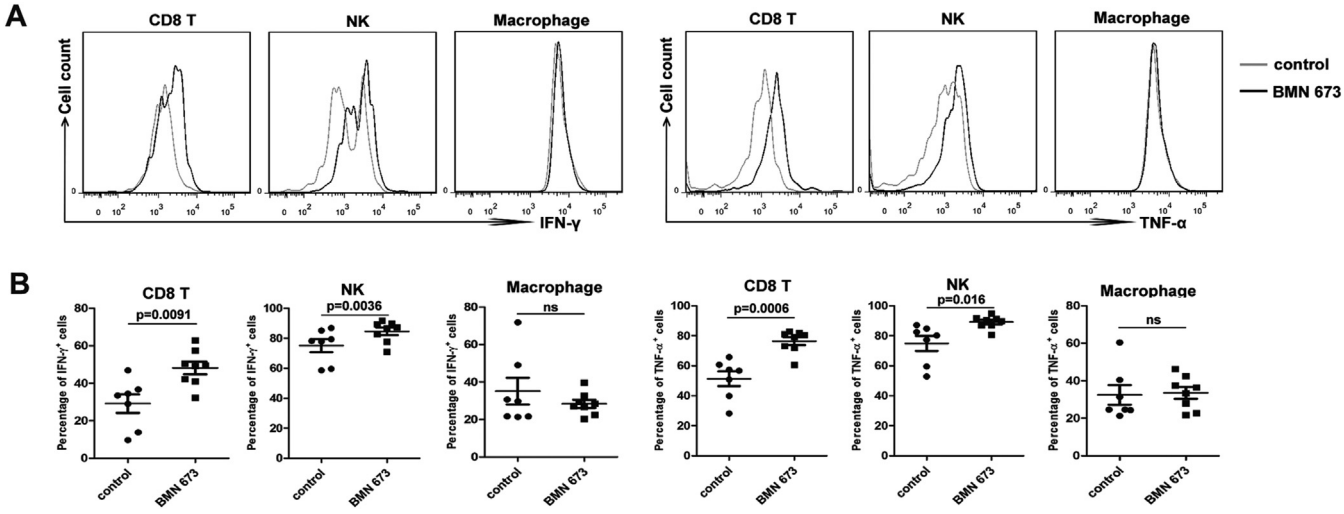

Fig. 4. BMN 673 treatment enhances the function of $CD8^+$ T cells and NK cells. FVB mice were inoculated i.p. with 4×10^6 BR5FVB1-Akt cells and then treated i.p. with PBS or 1 mg/kg BMN 673 on days 4, 6, 8, 10, and 12. On day 24 post tumor inoculation, a peritoneal wash was performed, and single-cell suspensions were analyzed by flow cytometry. Cell suspensions from the peritoneal wash were stimulated with PMA and ionomycin for 6 h, and stimulated cells were then analyzed for expression of IFN-γ and TNF-α in $CD8^+$ T cells, NK cells, or macrophages. (**A**) Representative results are shown for DMSO control- (gray) and BMN 673-treated (black) cells. **(B)** Quantitation of results from A with statistical results.

BMN 673 treatment increased production of IFN-γ and TNF-α by these cytotoxic lymphocytes. These cytokines play a critical role in surveillance against ovarian tumor development [21]. Indeed, immunodeficient mice that lack these molecules develop tumors spontaneously [22].

We also observed an increased percentage of tumor-associated $Foxp3^{+}CD4^{+}$ Tregs following BMN 673 treatment. The role of Tregs in ovarian cancer tissue remains unclear, as their presence has been associated with both decreased survival [11] and increased survival [23] among ovarian cancer patients. The impact of these cells may be contingent on other factors in the tumor microenvironment. Also, we evaluated the presence of Tregs in the peritoneal cavity rather than in tumor nodules, so the findings from the previous studies may not be directly comparable. Moreoever, any potential negative influence by Tregs seems to have been counterbalanced by the increased percentage of $CD8^{+}$ T cells. The ratio of $CD8^{+}$/Tregs is important to ovarian cancer patient survival [19], and this ratio remained unchanged despite the increase in Tregs.

BMN 673 is a potent member of an exciting new class of anticancer agents that exploit the biologic phenomenon of synthetic lethality as the basis for their antitumor selectivity. However, its clinical use is still in its infancy. Data herein reveal an immunoregulatory role for BMN 673 that may be critical to shaping antitumor immunity in the tumor-associated immunoenvironment. Further studies are expected to confirm that BMN 673 can be combined with existing and emerging immunotherapies to enhance their efficacy. Indeed, the efficacy of PD-1 pathway blockade correlates with DNA repair pathway mutations and neoantigen burden [24]. Thus, *BRCA*-deficient tumors are likely to be sensitive to such a combination therapy, and the inclusion of a PARP inhibitor is expected to produce even more neoantigens by further compromising DNA repair.

Conflicts of interest

The authors declare no conflicts of interest.

Acknowledgments

We thank the China Scholarship Council for its financial support of Dr. Jing Huang and Dr. Zhongyi Cong as well as the Susan Smith Center for Women's Cancer for its support of this work.

Transparency document

Transparency document related to this article can be found online at http://dx.doi.org/10.1016/j.bbrc.2015.05.083.

Appendix A. Supplementary data

Supplementary data related to this article can be found at http://dx.doi.org/10.1016/j.bbrc.2015.05.083.

References

[1] A. Jemal, R. Siegel, E. Ward, T. Murray, J. Xu, M.J. Thun, Cancer statistics, CA. Cancer J. Clin. 57 (2007) 43–66.
[2] B.T. Hennessy, R.L. Coleman, M. Markman, Ovarian cancer, Lancet 374 (2009) 1371–1382.
[3] K. Do, A.P. Chen, Molecular pathways: targeting PARP in cancer treatment, Clin. Cancer Res. 19 (2013) 977–984.
[4] C.J. Lord, A. Ashworth, The DNA damage response and cancer therapy, Nature 481 (2012) 287–294.
[5] M. Rouleau, A. Patel, M.J. Hendzel, S.H. Kaufmann, G.G. Poirier, PARP inhibition: PARP1 and beyond, Nat. Rev. Cancer 10 (2010) 293–301.
[6] M. Leung, D. Rosen, S. Fields, A. Cesano, D.R. Budman, Poly(ADP-ribose) polymerase-1 inhibition: preclinical and clinical development of synthetic lethality, Mol. Med. 17 (2011) 854–862.
[7] Y. Shen, F.L. Rehman, Y. Feng, J. Boshuizen, I. Bajrami, R. Elliott, et al., BMN 673, a novel and highly potent PARP1/2 inhibitor for the treatment of human cancers with DNA repair deficiency, Clin. Cancer Res. 19 (2013) 5003–5015.
[8] J. Murai, S.-Y.N. Huang, A. Renaud, Y. Zhang, J. Ji, S. Takeda, et al., Stereospecific PARP trapping by BMN 673 and comparison with olaparib and rucaparib, Mol. Cancer Ther. 13 (2014) 433–443.
[9] Z.A. Wainberg, J.S. de Bono, L. Mina, J. Sachdev, L.A. Byers, R. Chugh, et al., Abstract C295: update on first-in-man trial of novel oral PARP inhibitor BMN 673 in patients with solid tumors, Mol. Cancer Ther. 12 (2014). C295–C295.
[10] H. Qiu, Proteomic markers of DNA repair and PI3K pathway activation predict response to the PARP inhibitor BMN 673 in small cell lung cancer–letter, Clin. Cancer Res. 20 (2014) 2236.
[11] T.J. Curiel, G. Coukos, L. Zou, X. Alvarez, P. Cheng, P. Mottram, et al., Specific recruitment of regulatory T cells in ovarian carcinoma fosters immune privilege and predicts reduced survival, Nat. Med. 10 (2004) 942–949.
[12] M. Tomsová, B. Melichar, I. Sedláková, I. Steiner, Prognostic significance of CD3+ tumor-infiltrating lymphocytes in ovarian carcinoma, Gynecol. Oncol. 108 (2008) 415–420.
[13] D. Xing, S. Orsulic, A mouse model for the molecular characterization of brca1-associated ovarian carcinoma, Cancer Res. 66 (2006) 8949–8953.
[14] L. Zhang, N. Yang, J.-R.C. Garcia, A. Mohamed, F. Benencia, S.C. Rubin, et al., Generation of a syngeneic mouse model to study the effects of vascular endothelial growth factor in ovarian carcinoma, Am. J. Pathol. 161 (2002) 2295–2309.
[15] C. Marchetti, L. Imperiale, M.L. Gasparri, I. Palaia, S. Pignata, T. Boni, et al., Olaparib, PARP1 inhibitor in ovarian cancer, Expert Opin. Investig. Drugs 21 (2012) 1575–1584.
[16] E.Z. Zsiros, P. Duttagupta, D. Dangaj, H. Li, R. Frank, T. Garrabrant, et al., The ovarian cancer chemokine landscape is conducive to homing of vaccine-primed and CD3/CD28 costimulated T cells prepared for adoptive therapy, Clin. Cancer Res. (2015). Epub ahead of print.
[17] T.C.G.A.R. Network, Integrated genomic analyses of ovarian carcinoma, Nature 474 (2011) 609–615.
[18] S. Ostrand-Rosenberg, P. Sinha, Myeloid-derived suppressor cells: linking inflammation and cancer, J. Immunol. 182 (2009) 4499–4506.
[19] E. Sato, S.H. Olson, J. Ahn, B. Bundy, H. Nishikawa, F. Qian, et al., Intraepithelial CD8+ tumor-infiltrating lymphocytes and a high CD8+/regulatory T cell ratio are associated with favorable prognosis in ovarian cancer, Proc. Natl. Acad. Sci. U. S. A. 102 (2005) 18538–18543.
[20] M.A. Geller, S. Cooley, P.L. Judson, R. Ghebre, L.F. Carson, P.A. Argenta, et al., A phase II study of allogeneic natural killer cell therapy to treat patients with recurrent ovarian and breast cancer, Cytotherapy 13 (2011) 98–107.
[21] E.R. Kost, D.G. Mutch, T.J. Herzog, Interferon-gamma and tumor necrosis factor-alpha induce synergistic cytolytic effects in ovarian cancer cell lines-roles of the TR60 and TR80 tumor necrosis factor receptors, Gynecol. Oncol. 72 (1999) 392–401.
[22] S.E. Street, E. Cretney, M.J. Smyth, Perforin and interferon-gamma activities independently control tumor initiation, growth, and metastasis, Blood 97 (2001) 192–197.
[23] N. Leffers, M.J.M. Gooden, R.A. de Jong, B.-N. Hoogeboom, K.A. ten Hoor, H. Hollema, et al., Prognostic significance of tumor-infiltrating T-lymphocytes in primary and metastatic lesions of advanced stage ovarian cancer, Cancer Immunol. Immunother. 58 (2009) 449–459.
[24] N.A. Rizvi, M.D. Hellmann, A. Snyder, P. Kvistborg, V. Makarov, J.J. Havel, et al., Mutational landscape determines sensitivity to PD-1 blockade in non-small cell lung cancer, Science 348 (2015) 124–128.